Time-Dependent Electron Interactions in Double Rydberg Wave Packets

X. Zhang,[1] R. R. Jones,[1] and F. Robicheaux[2]
[1]Department of Physics, University of Virginia, Charlottesville, Virginia 22904-4714, USA
[2]Department of Physics, Auburn University, Alabama 36849, USA
(Received 9 September 2012; published 11 January 2013)

We investigate the time-dependent evolution of a nonstationary three-body Coulomb system at energies just below the threshold for three-body breakup. Experimentally, short-pulse lasers excite two electrons in Ba to radially localized Rydberg wave packets with well-defined energy and angular momentum. Time-dependent interactions between the two electrons are probed using half-cycle electric field pulses. The measurements indicate that substantial energy exchange between the two electrons is nearly immediate upon the launch of the second wave packet. Fully quantum and classical calculations support this observation, predicting extremely rapid autoionization under the experimental conditions. The calculations also show very fast angular momentum exchange and sensitivity to the relative binding energies of the two electrons.

DOI: 10.1103/PhysRevLett.110.023002 PACS numbers: 32.80.Rm, 32.80.Ee, 32.80.Qk, 32.80.Zb

Initiating dynamics in complex quantum systems can enable control of their internal interactions and can provide insights that are not obvious from frequency domain investigations. The prototype example of few-body dynamics in atomic physics is the interaction between two electrons within an atom. Electron-electron (e-e) interaction leads to correlation within bound states and autoionization from resonances that lie above the ionization threshold. Frequency domain approaches have afforded much understanding in cases where both electrons are tightly bound such that the e-e interaction leads to the coupling of relatively few independent electron channels, or when one electron is tightly bound and the other is highly excited so that the interaction is limited to a small volume near the atomic nucleus. However, when both electrons are highly excited the enormous density of states leads to nontrivial mixing, such that even qualitative features of the eigenstates can be difficult to predict. Experimentally, frequency domain spectroscopy fails to produce interpretable results as broad overlapping resonances and strong final-state mixing result in nearly featureless spectra [1–4]. Conversely, time-domain localization of the two-electron wave function allows one to intuitively explore complex correlated dynamics by viewing the system as it evolves through accessible channels [5–7]. In addition, the dynamics can be controlled by changing the initial characteristics of the wave packet [8,9].

Exploring two-electron dynamics remains a problem of great interest [10–12]. The principal experimental challenge is the identification of a time-resolved probe that can convey information about the evolving system at a specific instant in time, regardless of the two-electron wave packet configuration and absent final-state interactions that might alter the yields in measurement channels after the probe. Theoretically, time-domain studies at high energies require accurate calculations in the face of strong e-e interactions throughout a large volume and rapid changes in the wave function that persist over long times.

In this Letter we describe experimental and computational approaches that have enabled us to (i) create well-defined two-electron wave packets to perform the first direct measurements of time-dependent energy transfer at energies just below the threshold for three-body breakup, and (ii) calculate the evolution of double Rydberg wave packets (DRWs) using both classical and fully quantum methods. The experiment and calculations show that the radially localized configurations studied experimentally are extremely fragile, with substantial energy exchange occurring in a time less than half the orbit period for noninteracting electrons. The calculations also show that the initial wave packet with well-defined ℓ_1, ℓ_2 evolves to one with all allowed angular momenta in less than one period.

Figure 1 illustrates the situation investigated. Short laser pulses utilize isolated core excitation (ICE) [13] to sequentially excite the two valence electrons in Ba to coherent superposition states which initially resemble independent radial wave packets [14] associated with the neutral Ba atom and the singly charged Ba^+ ion, respectively. At their excitation, the energies (E_1 and E_2) and angular momenta (ℓ_1 and ℓ_2) of the two electrons are highly localized and, in the absence of the e-e interaction, would remain constant as the two wave packets evolve as decoupled, radially breathing shells. Of course, the two wave packets are not actually composed of pure neutral and ionic Rydberg states, respectively, and they do not move independently. Rather, the lasers coherently excite a continuum of highly correlated, two-electron states in which the energy and angular momentum of each electron are not well defined. The details of the superposition and its subsequent dynamics can be controlled by changing the frequencies and relative delays of the excitation laser pulses.

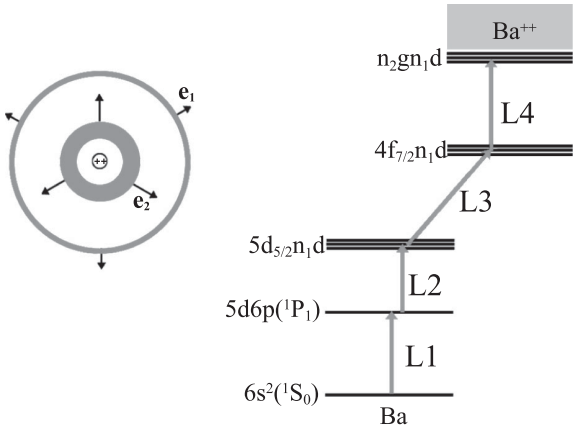

FIG. 1. Illustration of a radially localized DRW at a time soon after the second electron's excitation. Also shown is a schematic of the experimental DRW laser excitation.

In classical terms, energy and angular momenta transfer between the electrons occur with rates that depend on the relative proximity of the two electrons and the nucleus. Even if one electron obtains sufficient energy to leave the atom, autoionization may not occur immediately as subsequent e-e interactions can result in recapture. By changing the excitation energy and relative delay between the launch of the two wave packets, one can control the times of closest approach and, therefore, the two-electron dynamics.

Experimentally, ground-state Ba atoms in a thermal beam are exposed to a series of laser pulses to create $n_1 d n_2 g$ DRWs via a sequential, two-step, four photon process [6,7,15]. Here, $n_1 \sim 23$ and $n_2 \sim 38$ are the average effective principal quantum numbers of the first and second electrons in the neutral and ionic potentials, respectively. In the first step, atoms are excited from the $6s^2$ ground-state to the $5d6p\,^1P_1$ level using a 5-nsec laser pulse (L1). Immediately following the L1 pulse, a ~500-fsec, 528-nm laser pulse (L2) further excites the atoms to a coherent superposition of $5d_{5/2}n_1 d$ states with $20 < n < 26$ [16]. This radial wave packet (WP1) oscillates with a period of $\tau_1 \sim 1.8$ ps and has an outer turning point at $R_1 \sim 1100$ a.u.

The second excitation step is initiated at a variable time t_1 following the launch of WP1. A 300-fs, 233-nm pulse (L3) drives the first ICE, promoting the $5d_{5/2}n_1 d$ atoms to $4f_{7/2}n_1 d$ states. A ~500-fs, 313-nm laser pulse (L4), coincident with L3, completes the DRW excitation, performing a second ICE, $4f_{7/2}n_1 d \rightarrow n_2 g n_1 d$ $(34 < n_2 < 43)$ to create a radial wave packet (WP2) in the Ba^+ ion [15]. Absent energy exchange with the other electron WP2 would oscillate with a period of $\tau_2 \sim 2.1$ ps and an outer turning point of $R_2 \sim 1400$ a.u. Because $R_2 > R_1$, the two radial wave packets will eventually overlap and can exchange significant energy and angular momentum before the system has evolved for a time $\tau_2/2$. The delay t_1 determines the radial position of WP1 during the launch of WP2 and, accordingly, the radial distance from the ion and the time at which the wave packets first overlap [6,7].

The colinearly propagating, vertically polarized lasers are focused into the Ba beam between two parallel field plates in a time-of-flight spectrometer. Approximately 50 ns after the launch of WP2, a fast rising (~100 ns) voltage pulse is applied to the lower field plate. The resulting 2400-V/cm electric field pushes any ions in the interaction region toward a microchannel plate detector. The field has sufficient magnitude to diabatically ionize [17] the constituent Rydberg states of WP1 and >75% of the states ($n_2 > 37$) contributing to WP2. Consequently, in the absence of any e-e interaction, >75% of the double Rydberg atoms would be converted to Ba^{2+} ions via field ionization (FI). Far fewer Ba^{2+} ions are actually detected due to autoionization of the DRWs prior to the FI pulse. During autoionization, energy is transferred from one electron to the other, creating free electrons and tightly bound Rydberg ions which do not undergo FI to Ba^{2+}.

The principal goal of the experiments is to determine at what time(s), for different initial DRW configurations, energy transfer occurs between the two electrons. To this end, prior to the application of the FI pulse, the atoms are exposed to a 0.6-ps, half-cycle electric field pulse (HCP) polarized parallel to the excitation lasers with a peak amplitude of 7500 V/cm [18]. Because the duration of the HCP is shorter than the period of either wave packet, it can impulsively transfer momentum and energy to both Rydberg electrons [19–21]. The delay dependence of the HCP induced energy transfer provides a time-resolved probe of energy exchange between the electrons.

The effect of the HCP on the Ba^{2+} yield depends on its timing. Case 1: If the HCP appears before the excitation of WP1, it has no effect on the Rydberg dynamics and, due to autoionization of the DRW, the Ba^{2+} FI signal is small. Case 2: If the atoms interact with the HCP after the creation of WP1, but before the launch of WP2, there is a significant probability that WP1 will ionize. In this case, WP2 is a true ionic wave packet which cannot autoionize but, instead, field ionizes to produce a large Ba^{2+} yield. Case 3: If WP2 has been excited, but there has been negligible interaction between the two electrons, one or both electrons will likely be further excited or directly ionized by the HCP. The final ionic states produced via HCP ionization or subsequent autoionization lie well above the FI threshold and, similar to Case 2, a large Ba^{2+} signal is expected. Case 4: Since the energy needed to liberate one electron comes at the expense of the other, the average postautoionization Rydberg ion binding energy will be larger than in Cases 2 and 3. As a result, a HCP appearing after autoionization will excite fewer ions above the FI threshold, reducing the Ba^{2+} yield relative to Cases 2 and 3.

Figure 2(a) shows the Ba^{2+} FI yield as a function of the HCP delay relative to the excitation of WP1. Both plots

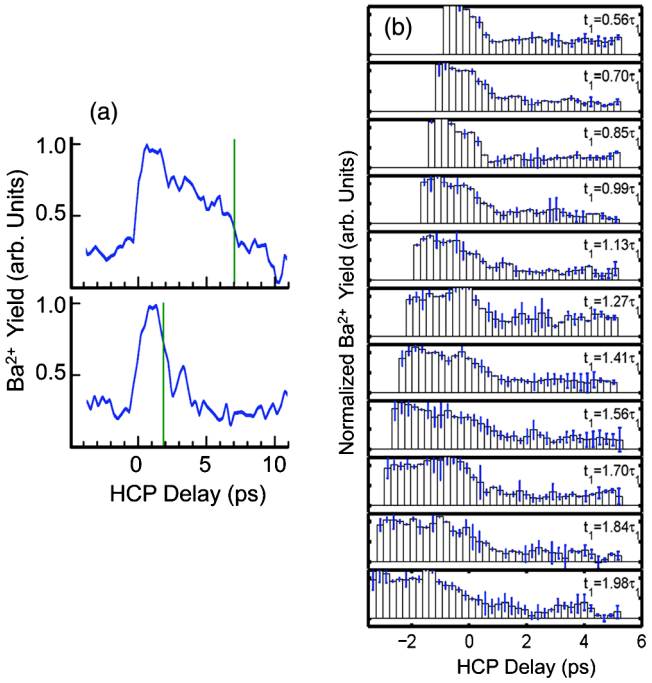

FIG. 2 (color online). (a) The measured Ba^{2+} signal versus HCP delay for different relative launch times for the two wave packets. The HCP delay is relative to the excitation of WP1 and the vertical green bars indicate the time of excitation of WP2, t_1. (b) Analogous to 2(a) except that the data are averaged over 230-fs time bins and normalized to the WP1 survival probability. The HCP delay is relative to the excitation of WP2. The delay t_1 of the WP2 excitation is noted (in units of τ_1) in each plot. The error bars are the standard deviation of two independent data runs.

clearly illustrate the expected rise in the Ba^{2+} signal as the HCP is scanned from before, to after, the excitation of WP1. The upper plot shows a slow ($\sim$7 ps) decay in the Ba^{2+} yield due to "stair-step" autoionization of WP1 [16,22–24]. This decay occurs prior to the creation of WP2 and simply reduces the DRW excitation probability. In the lower plot, negligible autoionization occurs before the launch of WP2, and a sharp decrease in the signal is observed at $t \sim t_1$. This reflects extremely rapid energy transfer between the electrons upon the launch of WP2, information which cannot be unambiguously inferred from frequency-domain absorption spectroscopy.

Data analogous to those shown in Fig. 2(a) have been collected for a range of t_1 values, such that the radial position of WP1 at t_1 varies from $r_1 \sim 0$ to $r_1 \sim R_1$ with both signs of radial velocity. To isolate the interesting Ba^{2+} signal changes that reflect DRW dynamics, rather than WP1 autoionization, the data in Fig. 2(b) have been normalized to the WP1 survival probability which is proportional to the Ba^{2+} yield obtained at large values of t_1 [upper plot in Fig. 2(a)]. All the normalized data have remarkably similar qualitative features; namely, within the temporal resolution of the experiment, all show a substantial signal decrease upon the excitation of WP2, in spite of the different initial conditions under which the data were collected. This indicates that energy exchange occurs very rapidly. Due to the large radial velocity of WP2 when it is launched, expansion to $0.7R_1$ occurs in only 0.2 ps. Thus the two wave packets can be found in relatively close proximity soon after the excitation, regardless of the radial position of WP1. The uniformity of the measurements indicates that complete spatial overlap between WP1 and WP2 is not required for energy transfer. This represents a refinement of a simple model of DRW autoionization as the result of the sudden change in ion-core screening that occurs when one wave packet passes through the other [6].

In an attempt to better understand the *e-e* dynamics underlying this observation, both quantum and classical simulations were performed. Several methods might be used to solve the time-dependent Schrödinger equation (e.g., see Refs. [25–27]). We used the modifications to the time-dependent close-coupling method [25] suggested in Ref. [28] due to the large spatial region of the wave function and the long propagation time. The calculations were performed using a split operator method with the individual propagators implemented using an implicit scheme. The implementation differs from that described in Ref. [28] in that the electrons are launched at negative energy using two Gaussian laser pulses. The bandwidths of the laser pulses are chosen so that the n-state distribution in each wave packet agrees with that in the experiment. The wave function is represented as a superposition of two-dimensional radial functions

$$\Psi(t) = \sum_i |i\rangle \mathcal{R}_i(r_1, r_2, t), \tag{1}$$

where $|i\rangle = |(\ell_1, \ell_2)L\rangle$ is the coupled angular momenta of the two electrons to give a specific total angular momentum L, and the $\mathcal{R}_i$ are tabulated on a two-dimensional grid of radial points. To simplify the calculation, we set $L = 0$. The experiments should be adequately described within this approximation since the dynamics for $n_1, n_2 \gg \ell_1, \ell_2$ are dominated by *e-e* interactions far from the nucleus where the wave packet probability distributions are insensitive to ℓ_1 and ℓ_2. We set $\ell_{\max} = 45$ in the calculation; the probability for the electron pair to be in a given ℓ decreased rapidly with ℓ beyond $\ell = 38$. In the results presented, the wave function was not symmetrized: electrons 1 and 2 were the first and second electrons launched, respectively. The calculations performed with singlet and triplet two-electron wave functions do not significantly differ from those shown. The calculations were performed in a radial region of 3000 a.u. with an absorbing mask for $r >$ 2000 a.u. to simulate autoionization. The first and second electrons do not reach the mask until their binding energies are reduced by factors of 2 and 1.5, respectively. As in the experiment, true autoionization cannot be distinguished from excitation to very weakly bound states.

Figure 3 shows the norm of the DRW versus time. In all of the plots, $t = 0$ corresponds to the center of the laser pulse exciting WP2. All curves show a steep drop followed by a plateau. The decrease is due to the mask which absorbs probability in the region $2000 < r < 3000$ a.u. The time when the norm drops depends on the mask location because of the electron travel time to the mask. The variation in the decay with respect to the different time delays depends on physics.

The drop occurs latest in time for $t_1 = \tau_1/2$. The *e*-*e* interaction is most gentle in this case since WP1 is at its outer turning point when WP2 is launched. There is relatively little energy exchanged so the electron travels slowly to the mask. The drop occurs earliest for $t_1 = \tau_1$ because the *e*-*e* interaction is strongest when both wave packets are simultaneously near the nucleus. In this case, there is a large energy exchange and the autoionized electron travels quickly to the mask. These two trends also are visible in the energy distribution of the Ba^+ states after autoionization; $t_1 = \tau_1/2$ gives the most weakly bound ions while $t_1 = \tau_1$ gives the most deeply bound ions. Importantly, after taking the different travel times to the mask into account, the numerical results are consistent with the rapid energy transfer indicated by the experiment.

The height of the plateau in the survival probability also depends on t_1, consistent with previous DRW experiments [6]. In particular, the DRW created with $t_1 = \tau_1/2$ has the largest probability of surviving the initial decay, while that for $t_1 = \tau_1$ is least likely to survive, correlating with whether the initial interaction between the electrons is strong or not. The difference between the curves at $t_1 = 3\tau_1/4$ and $t_1 = 5\tau_1/4$ suggests a dependence of the energy exchange on the relative electron velocities. WP1 is approximately at the same radius in the two cases, but for $t_1 = 3\tau_1/4$ it is moving toward the nucleus when the second electron is launched, while for $t_1 = 5\tau_1/4$ it is moving away.

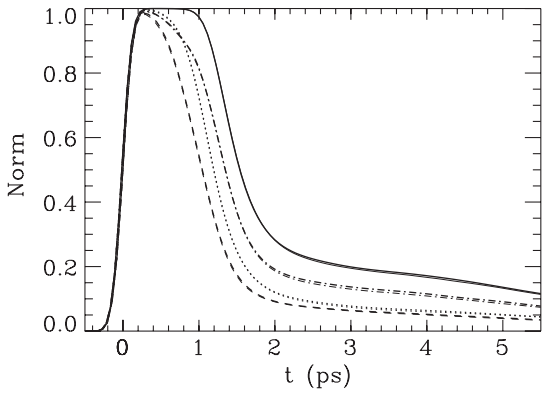

FIG. 3. DRW survival probability versus time for different delays between the laser pulses: $t_1 = \tau_1/2$ (solid line), $t_1 = 3\tau_1/4$ (dotted line), $t_1 = \tau_1$ (dashed line), $t_1 = 5\tau_1/4$ (dot-dash line). The quantum (bold line types) and classical (thin line types) results are barely distinguishable.

Calculations were performed for different energies of WP2, keeping the properties of WP1 fixed. We find substantially longer decay times and higher plateaus for slightly smaller values of n_2 (e.g., 32 instead of 38). This is partly because the two electrons approach and pass each other with somewhat less energy for smaller n_2, and partly because more energy transfer is required for the second electron to reach the mask. Interestingly, and in contrast to what is observed in the autoionization of single Rydberg states, the DRWs become more stable against autoionization as their excitation energy is decreased.

By performing quantum and classical calculations, we can determine if the classical approximation accurately describes this system. If so, relatively inexpensive classical computations can be used to interpret the quantum results and to explore a wider range of parameter space. The classical simulations mimic the quantum calculations as closely as possible. Both electrons were launched with Gaussian distributions in time and energy. The norm of the classical distribution was decreased whenever one of the electrons passed beyond $r = 2000$ a.u. Thus, there were no adjustable parameters to tweak the agreement between the quantum and classical calculations.

The classical time-dependent norms track the quantum norms within a few percent for the cases shown in Fig. 3. Moreover, we found that the norms classically computed for a distribution of trajectories with $0 \leq L \leq 4$ agreed well with those obtained for $L = 0$, supporting the validity of the quantum $L = 0$ approximation. The time-dependent classical and quantum angular momentum distributions did not track as well as the norms; while general trends were similar, differences up to $\sim$15% were found in some cases. These distributions show features as interesting as those of the norm. For example, the peak of the distribution can be near ℓ_1, $\ell_2 = 30$ for DRW propagation times less than τ_1. Since the largest classically allowed value is $\ell \sim 37$, this indicates maximal ℓ mixing on very short time scales.

In conclusion, we have performed experiments and calculations to directly explore controlled time-dependent electron-electron interactions in atoms. The measurements and calculations show that the initial wave packet configuration is extremely short lived, with substantial energy exchange occurring almost immediately upon the excitation of the second electron. The calculations indicate that angular momentum exchange is similarly rapid and, counterintuitively, that the autoionization rate decreases as the DRW is made slightly more bound. Future studies may take advantage of different laser polarizations, or excitation of oriented Stark states, to explore the evolution of DRWs with angular as well as radial localization in an attempt to identify longer-lived configurations.

This work was supported by the Chemical Sciences, Geosciences, and Biosciences Division of the Office of

Basic Energy Sciences, U.S. Department of Energy, and was made possible in part by a grant of high performance computing resources and technical support from the Alabama Supercomputer Authority.

[1] L. A. Bloomfield, R. R. Freeman, W. E. Cooke, and J. Bokor, Phys. Rev. Lett. **53**, 2234 (1984).
[2] P. Camus, T. F. Gallagher, J. -M. Lecomte, P. Pillet, L. Pruvost, and J. Boulmer, Phys. Rev. Lett. **62**, 2365 (1989).
[3] U. Eichmann, V. Lange, and W. Sandner, Phys. Rev. Lett. **64**, 274 (1990).
[4] R. R. Jones and T. F. Gallagher, Phys. Rev. A **42**, 2655 (1990).
[5] F. Robicheaux and R. C. Forrey, J. Phys. B **38**, S363 (2005).
[6] S. N. Pisharody and R. R. Jones, Science **303**, 813 (2004).
[7] S. N. Pisharody and R. R. Jones, Phys. Rev. Lett. **91**, 203002 (2003).
[8] B. J. Lyons, D. W. Schumacher, D. I. Duncan, R. R. Jones, and T. F. Gallagher, Phys. Rev. A **57**, 3712 (1998).
[9] R. R. Jones and L. D. Noordam, Adv. At. Mol. Opt. Phys. **38**, 1 (1998).
[10] S. Gilbertson, M. Chini, X. Feng, S. Khan, Y. Wu, and Z. Chang, Phys. Rev. Lett. **105**, 263003 (2010).
[11] J. Feist, S. Nagele, C. Ticknor, B. I. Schneider, L. A. Collins, and J. Burgdorfer, Phys. Rev. Lett. **107**, 093005 (2011).
[12] R. Pazourek, J. Feist, S. Nagele, and J. Burgdorfer, Phys. Rev. Lett. **108**, 163001 (2012).
[13] W. E. Cooke, T. F. Gallagher, S. A. Edelstein, and R. M. Hill, Phys. Rev. Lett. **40**, 178 (1978).
[14] A. ten Wolde, L. D. Noordam, A. Lagendijk, and H. B. van Linden van den Heuvell, Phys. Rev. Lett. **61**, 2099 (1988).
[15] X. Zhang and R. R. Jones, New J. Phys. **11**, 105050 (2009).
[16] X. Zhang, Ph.D. Dissertation, University of Virginia, 2008.
[17] T. F. Gallagher, *Rydberg Atoms* (Cambridge University Press, Cambridge, England, 1994), 1st ed., and references therein.
[18] D. You, R. R. Jones, D. R. Dykaar, and P. H. Bucksbaum, Opt. Lett. **18**, 290 (1993).
[19] R. R. Jones, D. You, and P. H. Bucksbaum, Phys. Rev. Lett. **70**, 1236 (1993).
[20] C. O. Reinhold, M. Melles, H. Shao, and J. Burgdorfer, J. Phys. B **26**, L659 (1993).
[21] A. Bugacov, B. Piraux, M. Pont, and R. Shakeshaft, Phys. Rev. A **51**, 4877 (1995).
[22] X. Wang and W. E. Cooke, Phys. Rev. Lett. **67**, 976 (1991).
[23] J. B. M. Warntjes, C. Wesdorp, F. Robicheaux, and L. D. Noordam, Phys. Rev. Lett. **83**, 512 (1999).
[24] J. E. Thoma and R. R. Jones, Phys. Rev. Lett. **83**, 516 (1999).
[25] M. S. Pindzola *et al.*, J. Phys. B **40**, R39 (2007).
[26] C. W. McCurdy, M. Baertschy, and T. N. Rescigno, J. Phys. B **37**, R137 (2004).
[27] K. Bartschat, E. T. Hudson, M. P. Scott, P. G. Burke, and V. M. Burke, J. Phys. B **29**, 115 (1996).
[28] F. Robicheaux, J. Phys. B **45**, 135007 (2012).